Supporting Information for:

Acoustic Coupling between Plasmonic Nanoantennas: Detection and Directionality of Surface Acoustic Waves

Martin Poblet,[†,‡,#] Rodrigo Berté,[¶,§,#] Hilario D. Boggiano,[†] Yi Li,[¶,‖] Emiliano Cortés,[¶] Gustavo Grinblat,[†] Stefan A. Maier,[*,¶,⊥] and Andrea V. Bragas[*,†]

†*Departamento de Física, FCEN, IFIBA CONICET, Universidad de Buenos Aires, C1428EGA Buenos Aires, Argentina*

‡*Current address: Catalan Institute of Nanoscience and Nanotechnology (ICN2), CSIC and BIST, Campus UAB, Bellaterra, 08193 Barcelona, Spain*

¶*Chair in Hybrid Nanosystems, Nanoinstitute Munich, Faculty of Physics, Ludwig-Maximilians-Universität München, 80539 München, Germany*

§*Instituto de Física, Universidade Federal de Goiás, 74001-970 Goiânia-GO, Brazil*

‖*Current address: School of Microelectronics, MOE Engineering Research Center of Integrated Circuits for Next Generation Communications, Southern University of Science and Technology, Shenzhen 518055, China*

⊥*Departament of Physics, Imperial College London, London SW7 2AZ, United Kingdom*

#*Contributed equally to this work*

E-mail: stefan.maier@physik.uni-muenchen.de; bragas@df.uba.ar

S1. Mechanical numerical simulations

Mechanical simulations were performed using the finite element method solver COMSOL Multiphysics by considering a linear elastic response of the isotropic materials and solving the Navier's equation in the frequency-domain:

$$\frac{E}{2(1+\nu)}\left[\frac{1}{1-2\nu}\nabla(\nabla\cdot\boldsymbol{u})+\nabla^2\boldsymbol{u}\right]+\boldsymbol{f}=\rho\frac{\partial^2\boldsymbol{u}}{\partial t^2}$$

where $\boldsymbol{u}$ is the displacement vector, $\boldsymbol{f}$ the force per unit volume generated by the thermal strain in the metal, ρ the mass density, E the Young's modulus and ν de Poisson's ratio of the material. Continuity of stress and displacement was considered between all boundaries. A perfectly matched layer was used to truncate the thickness of the glass substrate, simulating an infinite medium by absorbing propagating acoustic waves. A thermal strain, $\varepsilon_{\mathrm{th}}$, from the increase in the lattice temperature following the isotropic plasmon decay was considered for the displacive excitation mechanism that sets the particle in motion:

$$\varepsilon_{\mathrm{th}}=\alpha\,\Delta T$$

where α is the coefficient of thermal expansion and ΔT is the increment of the lattice temperature after pulsed laser excitation.

S2. Signal processing and statistical errors

Figure S1 shows the measured $\Delta T/T$ data on individual systems for representative sets of *direct signals* (left panel) and *delayed signals* (right panel). For each individual structure (or source-receptor pair, depending on the case) a series of 3 to 4 consecutive measurements is taken and then averaged resulting in the plotted gray curves. The average signal calculated from N identical systems is shown in red. For the temporal traces of single structures (gray curves), the standard deviation (gray-shaded bands), σ_{SD}, is associated with the background noise, whereas for the average signal (red curves), σ_{SD} mainly represents the dispersion in size, shape, adhesion to the substrate, etc., between the different measured systems. Red-shaded bands corresponds to the standard error of the mean, $\sigma_{\mathrm{SE}} = \sigma_{\mathrm{SD}}/\sqrt{N}$, and represents the standard deviation of the sample distribution for a set of N elements. With the aim of smoothing the data, a digital filter based on the Savitzky–Golay method was applied (2nd degree polynomial, 50 points wide window). The resulting smoothed average signals are displayed at the bottom of each panel.

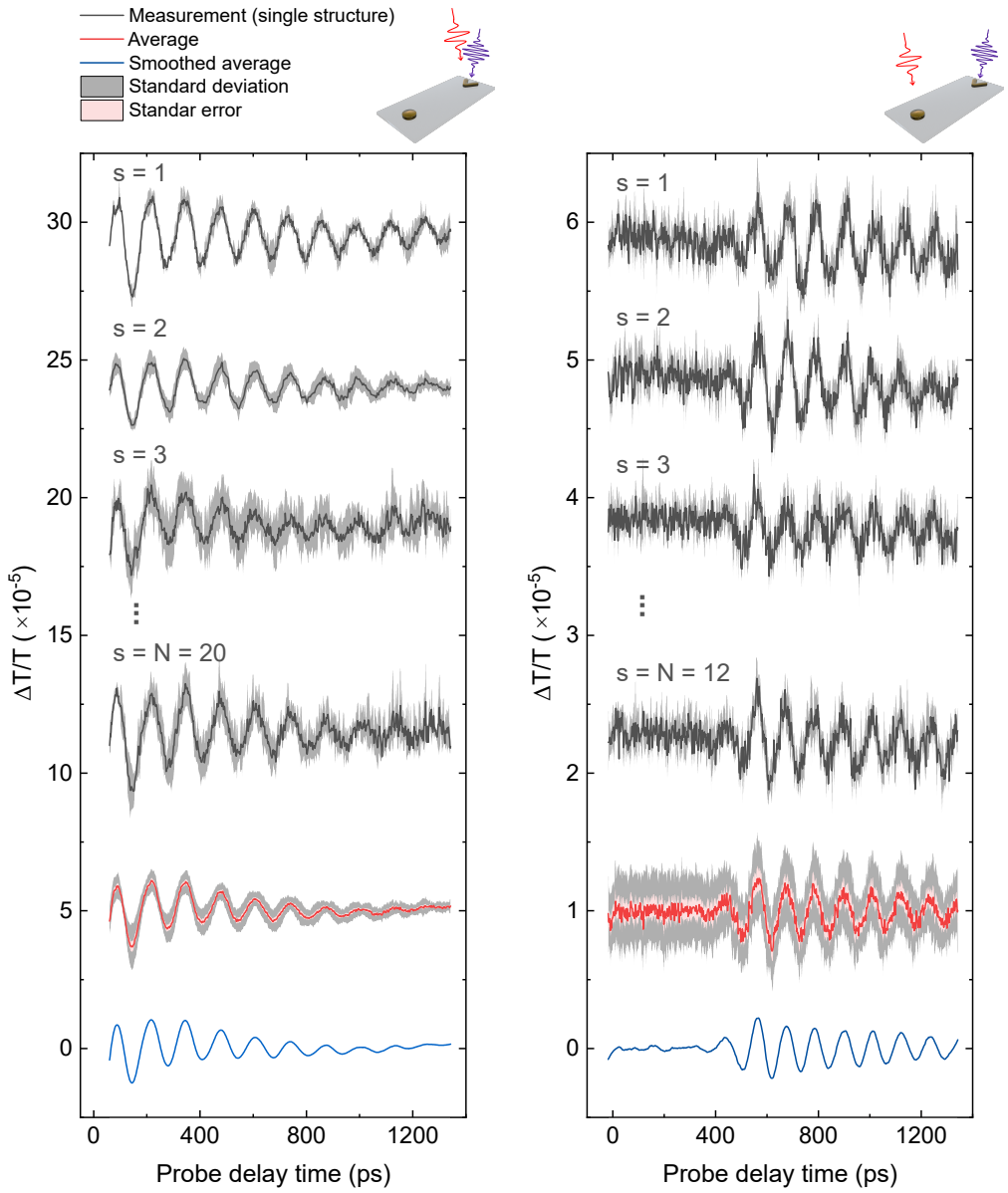

Figure S1: Signal processing and statistical errors. Differential probe transmission signals obtained from different individual systems (gray curves, labeled as $s = 1, 2, \ldots, N$) and the corresponding average curve (in red, the raw average signal, in blue, the smoothed one) for two different configurations: *direct signals* of V-shaped antennas and *delayed signals* with a V-shaped antenna as source and a disk as receptor ($\theta = 0$).

S3. Optical response of the Yagi-Uda antenna elements

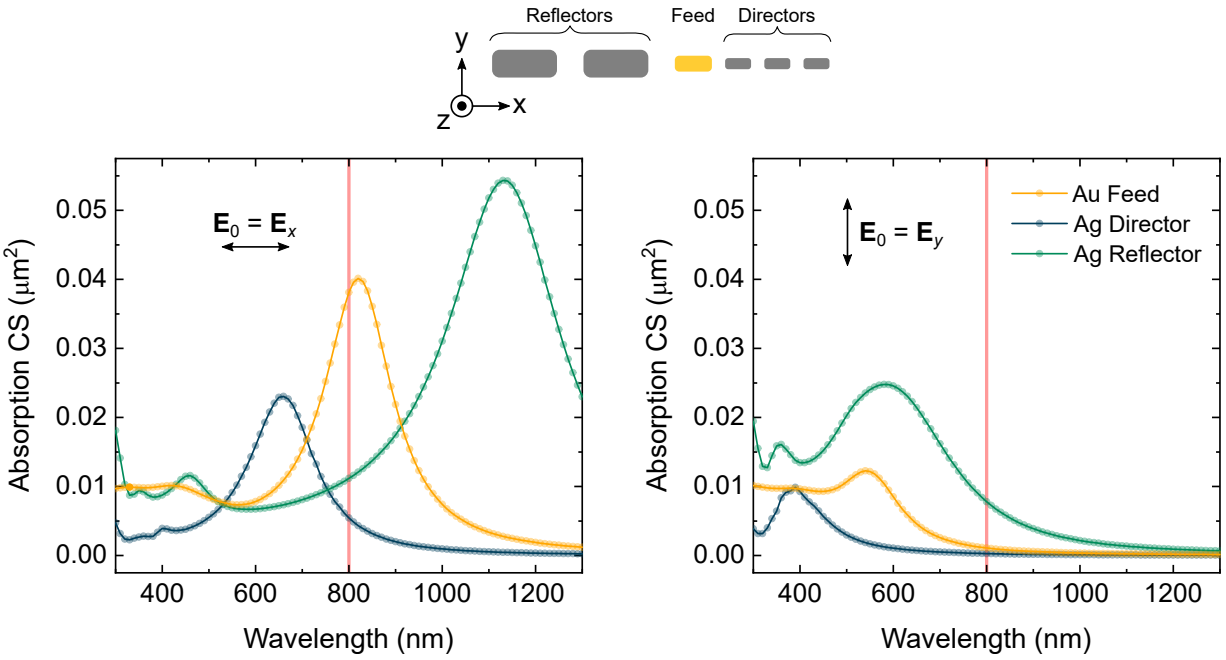

Figure S2: Simulated absorption cross section for the different components of the designed optomechanical Yagi-Uda nanoantenna. Arrows in the inset indicate the polarization of the incident electric field. The feed is a $140 \times 60 \times 35\,\text{nm}$ Au nanorod, and the reflector and director elements are $245 \times 105 \times 35\,\text{nm}$ and $98 \times 42 \times 35\,\text{nm}$ Ag rods, respectively. All the structures were designed with a 2 nm Cr adhesion layer on a glass substrate.

S4. Directional SAW emission by nano-mechanical Yagi-Uda antennas

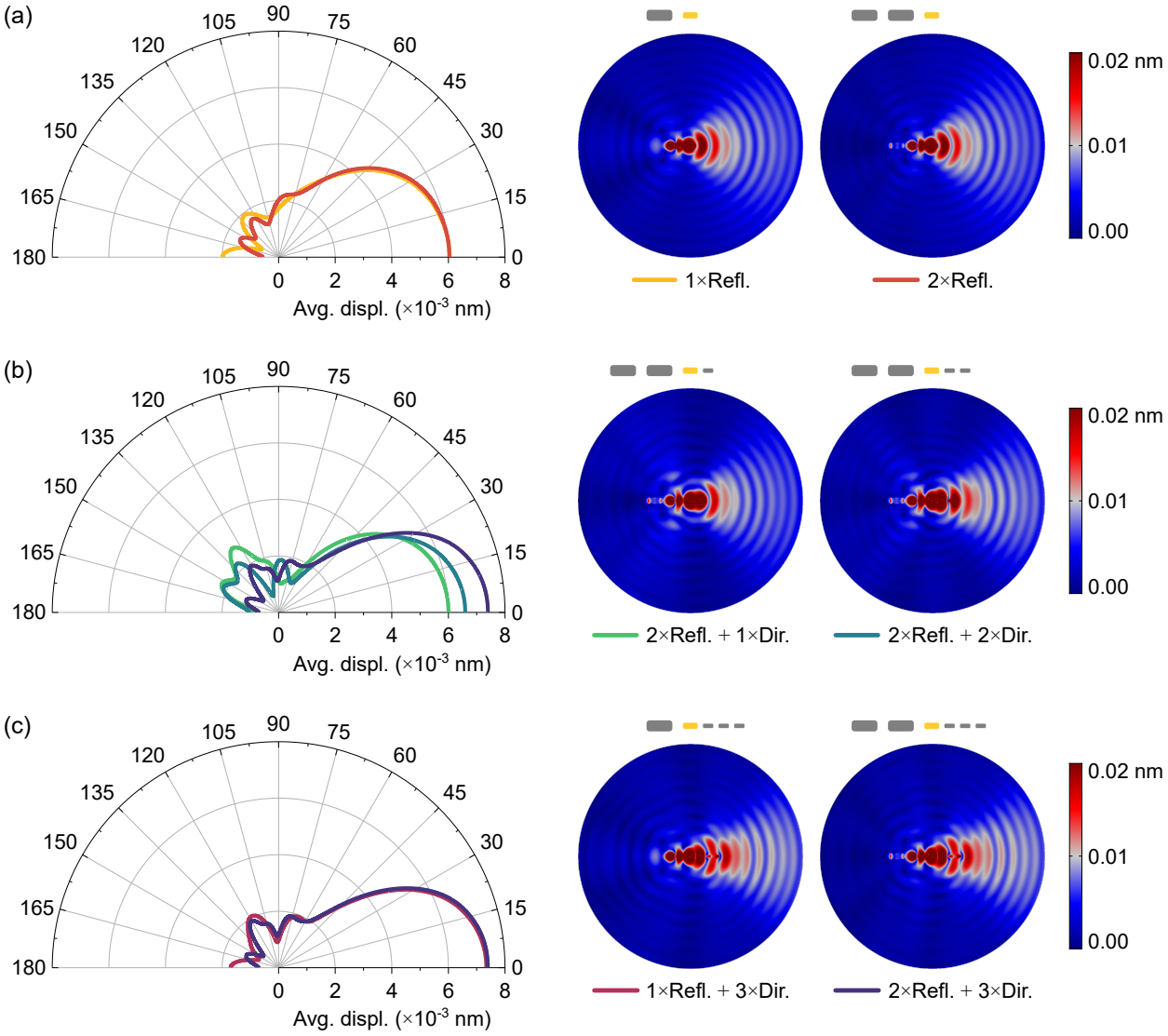

Figure S3: Acoustic emission pattern for different sets of passive components of the designed Yagi-Uda nanoantenna, obtained from FEM frequency-domain simulations. (a) Feed-rod with 1 or 2 reflectors. (b) Feed-rod with 2 reflectors and 1 to 3 directors. (c) Feed-rod with 3 directors and 1 or 2 reflectors. The polar graph at the left of each panel corresponds to the RMS radial displacement at the edge of the simulation domain (2 µm diameter), at 8.3 GHz, frequency of the main mode of oscillation of the gold feed (extensional mode, see Figure S5). The corresponding substrate displacement maps are shown on the right. The reflector spacing is $d_r = 100$ nm and the director spacing is $d_d = 50$ nm.

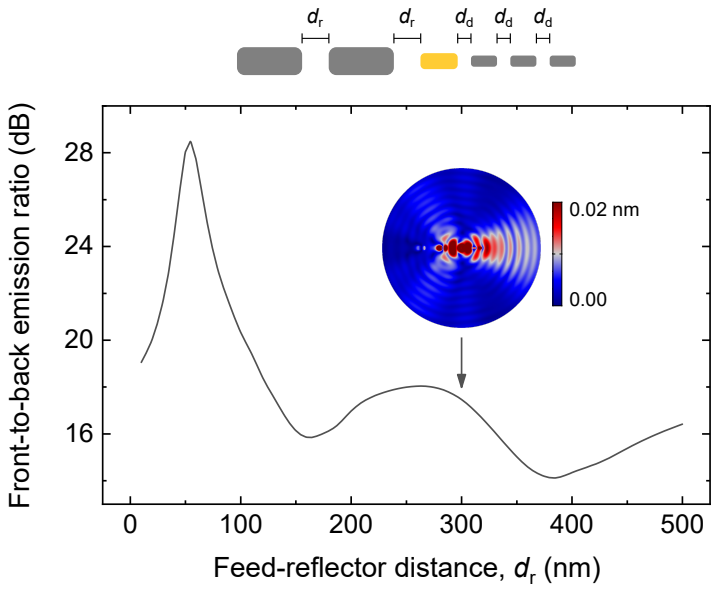

Figure S4: Front-to-back emission ratio as a function of the feed-reflector distance, d_r, at 8.3 GHz (frequency of the feed-rod extensional mode). This parameter is computed as $10 \times \log\left[(|\boldsymbol{u}_F|/|\boldsymbol{u}_B|)^2\right]$, where $|\boldsymbol{u}_{F/B}|$ is the forward/backward displacement amplitude obtained from FEM elastic simulations. The feed-director distance is fixed at $d_d = 50$ nm. The inset corresponds the substrate displacement pattern for $d_r = 300$ nm, showing that the Yagi-Uda antenna can maintain a significant directionality even when the distance between the feed and the reflector is increased.

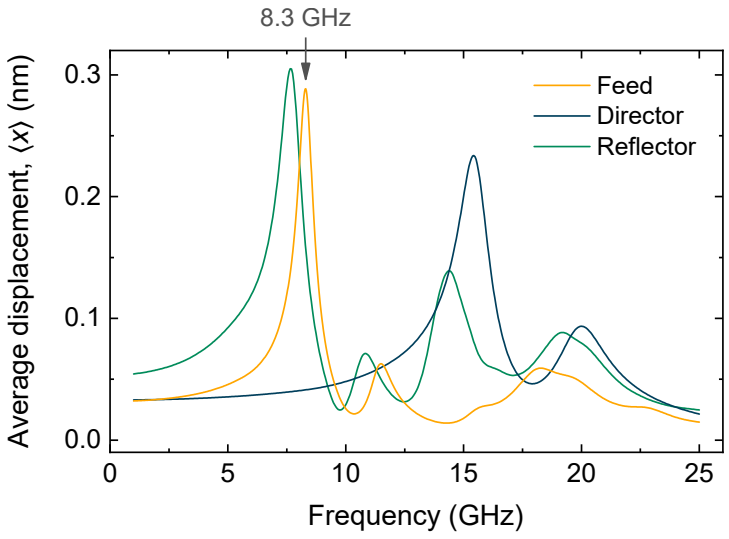

Figure S5: FEM frequency-domain simulations of the average displacement amplitude in the x-direction of the different Yagi-Uda antenna components separately as a function of strain frequency.